

# Enhancing the Computational Efficiency of the DoNOF Program through a New Orbital Sorting Scheme

Élodie Boutou<sup>1,2,3</sup>, Juan Felipe Huan Lew-Yee<sup>3</sup>, Jose Maria Mercero<sup>1,3</sup>,  
Mario Piris<sup>1,3,4</sup>

<sup>1</sup>*Kimika Fakultatea, Euskal Herriko Unibertsitatea (UPV/EHU), 20018 Donostia, Spain.*

<sup>2</sup>*Polytech Clermont, University of Clermont Auvergne, 63178 Aubière Cedex, France.*

<sup>3</sup>*Donostia International Physics Center (DIPC), 20018 Donostia, Spain.*

<sup>4</sup>*Basque Foundation for Science (IKERBASQUE), 48013 Bilbao, Spain.*

---

## Abstract

This work presents a novel approach to distribute orbitals into subspaces within electron-pairing-based natural orbital functionals (NOFs). This approach modifies the coupling between weakly and strongly occupied orbitals by applying an alternating orbital sorting strategy. In contrast to the previous orbital sorting that enforced electron pairing within subspaces of contiguous orbitals, the new approach provides greater flexibility, enabling a calculation scheme where the size of the subspaces can be gradually expanded. As a consequence, one can start using subspaces of only one weakly occupied orbital (perfect pairing) and progressively enlarge their size by incorporating more weakly occupied orbitals (extended pairing) up to the maximum size allowed by the basis set. In this way, the alternate orbital sorting allows solving first a simpler problem with small subspaces and leverage its orbital solution for the more intensive problem with larger subspaces, thereby reducing the overall computational cost and improving convergence, as we observed in the DoNOF program. The efficiency provided by the new sorting approach has been validated through benchmark calculations in  $\text{H}_2\text{O}$ ,  $\text{H}_2\text{O}_2$ , and  $\text{NH}_3$ . In

---

*Email addresses:* [elodie.boutou@etu.uca.fr](mailto:elodie.boutou@etu.uca.fr) (Élodie Boutou<sup>1,2,3</sup>),  
[felipe.lew.yee@dipc.org](mailto:felipe.lew.yee@dipc.org) (Juan Felipe Huan Lew-Yee<sup>3</sup>), [jm.mercero@ehu.eus](mailto:jm.mercero@ehu.eus) (Jose Maria Mercero<sup>1,3</sup>), [mario.piris@ehu.eus](mailto:mario.piris@ehu.eus) (Mario Piris<sup>1,3,4</sup>)

particular, we compared three strategies: i) solving directly the calculation with the largest subspaces (one-shot strategy), as was usually done before this work, ii) starting with perfect pairing and stepwise increasing the number of orbitals in the subspaces one by one until reaching the maximum size (incremental strategy), and iii) starting with perfect pairing and transitioning directly to the maximum subspace size (two-step strategy). Our results show that the two-step approach emerges as the most effective strategy, achieving the lowest computational cost while maintaining high accuracy. These results confirm that the alternating orbital sorting scheme provides a robust and scalable framework for improving NOF calculations and could be particularly advantageous for extending these methods to larger and strongly correlated systems.

*Keywords:* Natural Orbital Functional Theory, Optimization, DoNOF

---

## 1. Introduction

In recent years, Natural Orbital Functional Theory (NOFT) [1–5] has emerged as a powerful framework to describe electron correlation [6]. Unlike traditional wavefunction-based approaches, which often suffer from steep computational scaling, NOFT provides a formally fifth-order scaling, which can be reduced to fourth-order [7–9], making it significantly more efficient while maintaining an accurate description of correlated electronic states. This efficiency advantage is particularly relevant for multireference systems, where NOFT provides deeper insights than density functional approximations [10–18]. By circumventing the limitations of conventional multireference methods, which rely on small active spaces and quickly become computationally intractable, NOFT enables the treatment of larger correlated electron systems while maintaining accuracy.

Beyond its success in ground-state electronic structure calculations, NOFT has been extended to describe excited states and molecular dynamics, broadening its applicability to time-dependent phenomena. Recent developments have demonstrated that NOFT can accurately capture excited-state properties by coupling natural orbital functionals with the extended random phase approximation (ERPA) [19, 20]. These advances enable a systematic treatment of excited-state correlation effects, offering an alternative to traditional time-dependent density functional theory (TDDFT) or multireference wavefunction methods, particularly for strongly correlated systems. In addition,

the application of NOFT to ab initio molecular dynamics (AIMD) has provided new insights into electronic structure evolution in real-time simulations, demonstrating its ability to describe dynamic electron correlation effects [21, 22]. Furthermore, NOFT has shown remarkable improvements in addressing delocalization errors, a common challenge in density functional theory (DFT) that impacts the accuracy of charge transfer and reaction energy calculations [23].

Despite these advances, further optimization of NOFT methods is necessary to enhance computational performance and extend applicability to more complex systems. A key development in this direction has been the incorporation of modern numerical techniques inspired by deep learning [24], which have significantly improved the convergence behavior of NOF calculations. In particular, the introduction of momentum-based techniques such as the ADAM optimizer for natural orbital optimization has led to substantial speed-ups in reaching self-consistency. Reference [24] demonstrated the impact of these advances by presenting the largest NOF calculations to date, including a 1000-electron hydrogen cluster, a system that would be computationally prohibitive for conventional wavefunction-based methods. By representing the electronic structure in terms of natural orbitals [25] and their corresponding occupation numbers, NOFT provides a distinct and comprehensive perspective on electron correlation, leading to the development of various functionals with different correlation treatments, as reviewed in [26–29].

Among these developments, Piris natural orbital functionals (PNOFs) [30–39] have emerged as a highly effective realization of NOFT, offering a balance between accuracy and computational efficiency. These functionals explicitly incorporate electron correlation while ensuring necessary ensemble  $N$ -representability conditions [40]. For a long time, pure and ensemble universal functionals were believed to be equivalent within the domain of pure-state  $N$ -representable 1RDMs [41]. However, more recent studies [42] revealed that the ensemble functional is actually the lower convex envelope of the pure functional, highlighting a fundamental distinction between the two. Fortunately, their equivalence was later confirmed on the set of  $v$ -representable 1RDMs [43], ensuring that for ground-state electronic systems under an external potential  $v(\mathbf{r})$ , pure and ensemble functionals are indistinguishable. As a result, we can impose only ensemble constraints during the energy minimization process, simplifying the enforcement of  $N$ -representability conditions.

PNOFs leverage the exact functional of the two-particle reduced density

matrix ( $D$ ) [44], requiring only the reconstruction  $D[n_i, n_j, n_k, n_l]$  from the occupation numbers, leading to the following general form:

$$E[\{n_i, \phi_i\}] = \sum_i n_i H_{ii} + \sum_{ijkl} D[n_i, n_j, n_k, n_l] \langle kl|ij \rangle \quad (1)$$

where  $n_i$  denotes the occupation number of the natural spin orbital  $\phi_i$ . The term  $H_{ii}$  represents the one-particle Hamiltonian matrix elements, including kinetic energy and potential energy contributions:

$$H_{ii} = \int d\mathbf{r} \phi_i^*(\mathbf{r}) \left( -\frac{\nabla^2}{2} + v(\mathbf{r}) \right) \phi_i(\mathbf{r}) \quad (2)$$

while  $\langle kl|ij \rangle$  denotes the two-particle interaction matrix elements, given by:

$$\langle kl|ij \rangle = \iint d\mathbf{r}_1 d\mathbf{r}_2 \frac{\phi_k^*(\mathbf{r}_1) \phi_l^*(\mathbf{r}_2) \phi_i(\mathbf{r}_1) \phi_j(\mathbf{r}_2)}{|\mathbf{r}_2 - \mathbf{r}_1|} \quad (3)$$

The success of PNOFs lies in the fact that  $D$  satisfies 2-positivity necessary ensemble N-representability conditions [45] and is reconstructed in terms of two-index auxiliary matrices, leading to JKL-only functionals of the following form:

$$E = 2 \sum_p n_p H_{pp} + \sum_{pq} A[n_p, n_q] J_{qp} - \sum_{pq} B[n_p, n_q] K_{qp} - \sum_{pq} C[n_p, n_q] L_{qp} \quad (4)$$

where  $J_{qp}$ ,  $K_{qp}$ , and  $L_{qp}$  represent the usual Coulomb, exchange, and exchange-time-inversion integrals [46, 47], respectively. Note that the indices here refer to natural spatial orbitals, and their occupancies  $\{n_p\}$  determine the functions  $A$ ,  $B$ , and  $C$ . The fundamental features of these functionals have previously been analyzed in several review articles [48–50].

Notably, the PNOFs based on electron pairing have demonstrated significant potential [51] due to their ability to directly incorporate both dynamic and static correlation effects, allowing for a more accurate and computationally efficient description of strongly correlated systems. Within this framework, four functionals stand out: PNOF5 [34, 35], PNOF6 [36], PNOF7 [37, 38], and the recently proposed global NOF (GNOF) [39]. The electron-pairing methodology divides electron correlation into intrapair and interpair components. PNOF5 is an N-representable functional that accounts for intrapair electron correlation, while PNOF7 extends this description by including static interpair electron correlation effects. PNOF6, on the other hand,

considers both intrapair and interpair correlations but fails to capture a significant portion of the correlation energy. GNOF addresses this limitation by incorporating dynamic interpair electron correlation, achieving a balance between static and dynamic correlation effects. Additional information on GNOF for singlet states, which are the only states considered in this work, can be found in the Appendix.

PNOF calculations can be performed using the DoNOF program [52], an open-source software written in Fortran. This program is specifically designed to address the energy minimization problem for the ground-state energy (4), adhering to the orthonormality constraints of the natural orbitals and the electron-pairing restrictions on the occupation numbers. Importantly, these pairing constraints inherently satisfy the ensemble N-representability conditions of the one-particle reduced density matrix [53]. The optimization process is carried out in two interconnected stages, where the energy is independently optimized with respect to the occupation numbers and natural orbitals. Orbital optimization is achieved using either the iterative diagonalization method [54] or the adaptive momentum technique recently introduced for this purpose [24]. Additionally, specialized parameterizations have been developed [55] to comply with the pairing constraints, enabling unconstrained optimization of the occupation numbers. These two stages are iteratively executed in an integrated process until convergence is reached for both the occupation numbers and the natural orbitals.

Despite the physical advantages of the electron-pairing scheme, its current implementation with orbitals of a space being contiguous imposes an artificial limitation, restricting flexibility in adjusting the number of orbitals coupled within subspaces to ensure electron pairing. This sorting makes it impossible to reuse previous calculations when the size of the electron-pairing scheme is increased. This work overcomes this drawback by introducing an alternative orbital sorting approach that alternates the sequence of orbital coupling. The proposed method retains the functional definitions while providing greater flexibility in defining subspaces. Notably, it enables the reuse of previously converged solutions for subsequent calculations, facilitating seamless adjustments to the number of coupled orbitals, whether increasing or decreasing them as required.

In this study, we compare the original coupling strategy, here referred to as “continuous orbital sorting”, with the new “alternating orbital sorting”. The proposed approach is validated through calculations on  $\text{H}_2\text{O}$ ,  $\text{H}_2\text{O}_2$  and  $\text{NH}_3$ , focusing on computational time and iteration count. We evaluated

three scenarios: (i) a one-shot calculation, the “old” way, where the PNOF computation is performed directly with the maximum number of coupled orbitals; (ii) an incremental approach, starting with a single coupled orbital and gradually increasing the number up to the maximum; and (iii) a two-step calculation, which begins with a single coupled orbital and then directly transitions to the maximum number of coupled orbitals. The latter two approaches, made possible by the new coupling strategy, demonstrate significant improvements in both efficiency and flexibility.

## 2. Algorithm

Typically, we consider  $N_I$  unpaired electrons, which determine the total spin of the system  $S$ . The remaining electrons,  $N_{II} = N - N_I$ , form electron pairs with opposite spins, resulting in a net spin of zero for the paired electrons. For the mixed state with the highest multiplicity, defined by  $2S+1 = N_I+1$ , the expected value of  $\hat{S}_z$  is zero. As a result, the restricted spin formalism is applied, where  $n_p^\alpha = n_p^\beta = n_p$  [56].

In line with  $N_I$  and  $N_{II}$ , the orbital space  $\Omega$  is divided into two subspaces:  $\Omega = \Omega_I \oplus \Omega_{II}$ .  $\Omega_{II}$  is composed of  $N_{II}/2$  mutually disjoint subspaces  $\Omega_g$ . Each of which contains one strongly occupied orbital  $|g\rangle$  with  $g \leq N_{II}/2$ , and  $N_g$  weakly occupied orbitals  $|p\rangle$  with  $p > N_{II}/2$ , namely,

$$\Omega_g = \{|g\rangle, |p_1\rangle, |p_2\rangle, \dots, |p_{N_g}\rangle\}. \quad (5)$$

Taking into account the spin, the total occupancy for a given subspace  $\Omega_g$  is 2, which is reflected in the following  $N_{II}/2$  pairing conditions:

$$\sum_{p \in \Omega_g} n_p = n_g + \sum_{i=1}^{N_g} n_{p_i} = 1, \quad g = 1, 2, \dots, \frac{N_{II}}{2}. \quad (6)$$

In general,  $N_g$  can vary across subspaces as long as it adequately describes the electron pair. However, for simplicity,  $N_g$  is assumed to be the same for all subspaces  $\Omega_g \in \Omega_{II}$ . The maximum allowable value of  $N_g$  is determined by the basis set employed in the calculations. From (6), the following expression holds:

$$2 \sum_{p \in \Omega_{II}} n_p = 2 \sum_{g=1}^{N_{II}/2} \left( n_g + \sum_{i=1}^{N_g} n_{p_i} \right) = N_{II}. \quad (7)$$

Similarly,  $\Omega_I$  is composed of  $N_I$  mutually disjoint subspaces  $\Omega_g$ . Unlike  $\Omega_{II}$ , each subspace  $\Omega_g \in \Omega_I$  contains only one orbital  $g$  with  $n_g = 1/2$ . As expected, the orbitals in  $\Omega_I$  are not subject to the pairing condition, since each is singly occupied by an electron. However, the specific spin state of these electrons, whether  $\alpha$  or  $\beta$  remains indeterminate. Consequently, we have:

$$2 \sum_{p \in \Omega_I} n_p = 2 \sum_{g=N_{II}/2+1}^{N_{II}/2+N_I} n_g = N_I. \quad (8)$$

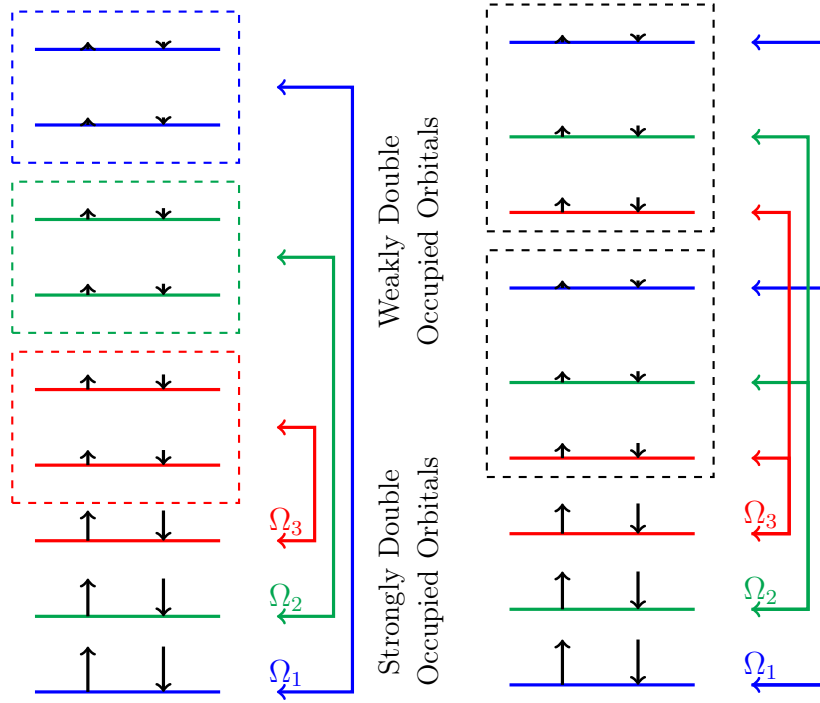
Taking into account Eqs. (7) and (8), the trace of the one-particle reduced density matrix is verified to be equal to the number of electrons:

$$2 \sum_{p \in \Omega} n_p = 2 \sum_{p \in \Omega_{II}} n_p + 2 \sum_{p \in \Omega_I} n_p = N_{II} + N_I = N. \quad (9)$$

From this point forward, we will focus on the subspace  $\Omega_{II}$ , as it is the one affected by the pairing conditions, whose implementation will be modified. Figure 1 provides an illustrative example. In this case,  $N_I = 0$  ( $S = 0$ ), indicating the absence of singly occupied orbitals, while six electrons ( $N_{II} = 6$ ) are distributed across three subspaces,  $\Omega_1, \Omega_2, \Omega_3$ , which collectively constitute  $\Omega_{II}$ . In this example,  $N_g = 2$  corresponds to the weakly occupied orbitals, which are depicted within the dashed-line boxes and are paired within each subspace  $\Omega_g$  to the strongly occupied orbitals shown in the lower lines.

It is important to recall that the orbitals belonging to each subspace  $\Omega_g$  vary throughout the optimization process until the most favorable orbital interactions are found. As a result, they do not remain fixed but adapt to the specific problem at hand, regardless of the starting orbitals used in the calculation. This means that the order in which the weakly occupied orbitals are selected to form the subspaces  $\Omega_g$  does not affect the physical nature of the problem. However, it can influence the number of iterations and consequently the time required to obtain the optimal orbitals.

The simplest way to construct a subspace  $\Omega_g$  is to select the  $N_g$  weakly occupied orbitals coupled to a strongly occupied orbital in a continuous manner, as illustrated in the dashed-line boxes in Figure 1a. However, this continuous ordering introduces an artificial barrier when changing  $N_g$  for a new calculation. For example, in Figure 1a, where  $N_g = 2$ , restarting the calculation with  $N_g = 1$  using the previously converged orbitals from the  $N_g = 2$  calculation as starting orbitals causes the second orbital in  $\Omega_3$  to shift into  $\Omega_2$ ,



(a) Continuous Orbital Sorting (Old)

(b) Alternating Orbital Sorting (New)

Figure 1: Graphical depiction of continuous orbital sorting and the alternating orbital sorting. In this example,  $N_I = 0$  ( $S = 0$ ), whereas six electrons ( $N_{II} = 6$ ) distributed in three subspaces  $\Omega_1, \Omega_2, \Omega_3$  make up the subspace  $\Omega_{II}$ . Note that  $N_g = 2$ . The arrows represent the occupation numbers for alpha ( $\uparrow$ ) and beta ( $\downarrow$ ) spins in each orbital

discarding the previously converged orbital in  $\Omega_2$ . Comparable situations will occur when, instead of decreasing  $N_g$  for a new calculation, the number of coupled orbitals is increased. Consequently, several additional iterations will be needed to regain convergence.

This issue can be addressed by using an alternating orbital sorting method. As illustrated in Figure 1b, we assign the first weakly occupied orbital to  $\Omega_3$ , the next one to  $\Omega_2$ , and the following one to  $\Omega_1$ . This process is repeated  $N_g$  times. Since each dashed-box in the Figure 1b contains an orbital from each subspace, adjusting the number of coupled orbitals in a subspace (either fewer or more) corresponds to reducing or increasing the number of dashed-boxes, respectively. This approach allows us to reuse the previously converged orbitals, which ultimately enhances the efficiency of the calculation.



### 3. Results

In this section, we present the results obtained using GNOF [39], our latest functional designed to achieve a balanced treatment of static and dynamic correlation effects. Orbital optimization was performed with the recently implemented adaptive momentum technique [24], while the unconstrained optimization of occupation numbers was performed using the softmax parametrization [55], ensuring compliance with the pairing constraints. All calculations were performed using experimental geometry and correlation-consistent cc-pVTZ basis sets developed by Dunning and coworkers [57]. A parallel version of the DoNOF software was used on 0na AMD Ryzen 5 4600H CPU.

The water molecule is one of the most studied systems in quantum chemistry, making it an ideal candidate for examining how subspace size influences electronic structure calculations. It also provides a suitable benchmark to assess the performance of the new alternating orbital sorting implemented in the DoNOF program [52] compared to continuous orbital sorting. As a benchmark system, water enables a systematic investigation of how subspace size affects the convergence behavior and accuracy of NOF calculations, as well as how increasing the number of weakly occupied orbitals impacts the recovery of electron correlation. To illustrate this, we calculated the energy of water for different values of  $N_g$ , recalling that  $N_g$  represents the number of weakly occupied orbitals coupled with strongly occupied ones in each subspace. The effect of subspace size on the total electronic energy is depicted in Figure 2, where each point corresponds to an independent one-shot calculation, which means that the optimization was performed from scratch for each selected value of  $N_g$ .

In the simplest case, where only one weakly occupied orbital is coupled with a strongly occupied orbital in each subspace ( $N_g = 1$ ), the calculation predominantly captures static correlation effects. This scenario, known as perfect pairing, maximizes the fractional occupation of the weakly occupied orbital while ensuring strict electron pairing. In systems dominated by static correlation, such as dissociations or diradical species, this configuration provides an accurate description of the electronic structure, with weakly occupied orbitals reaching half-occupation. However, for systems where dynamic correlation is significant, perfect pairing alone is insufficient, as it fails to describe the finer energy contributions arising from electron interactions beyond strictly paired orbitals.

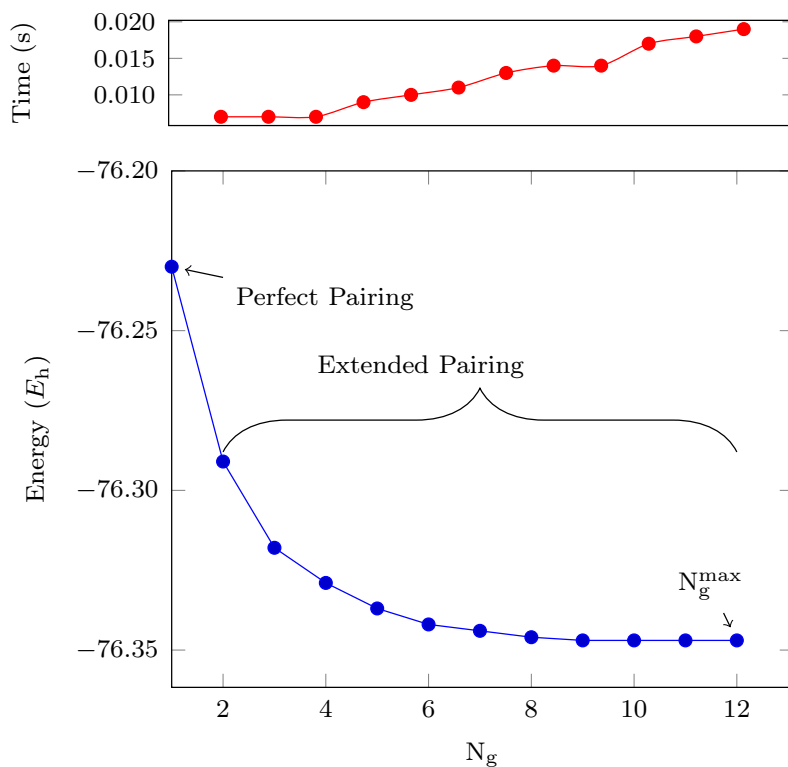


Figure 2:  $H_2O$  calculated using GNOF/cc-pVTZ as a function of the subspace. The one-shot scheme was employed, that is, each point has been computed independently. Top panel shows the time per orbital iteration, while bottom panel shows the energy for each subspace size.

To recover these missing correlation effects, it is necessary to expand the subspace by incorporating additional weakly occupied orbitals ( $N_g > 1$ ). This extension follows the extended pairing scheme, where more orbitals participate in the correlation process, enabling a more balanced description of both static and dynamic contributions. As shown in Figure 2, increasing  $N_g$  systematically lowers the electronic energy, reflecting the gradual recovery of correlation energy. While larger subspaces improve accuracy, they also increase computational cost, as the number of variational parameters and required optimization steps grows significantly.

The results shown in Figure 2 underscore the fundamental role of the subspace size in capturing electron correlation effects within NOFT. Ideally, the highest accuracy is achieved when the maximum number of orbitals allowed by the basis set is included. For the  $\text{H}_2\text{O}$  molecule with the cc-pVTZ basis set, this corresponds to  $N_g^{\text{max}} = 12$ . The observed energy trend confirms that increasing  $N_g$  systematically improves the accuracy of the electronic structure description by incorporating more dynamic correlation. However, this improvement comes at the cost of increased computational effort, highlighting the need for efficient strategies to optimize orbital selection and convergence. Although the results presented here were obtained using the one-shot scheme, they establish a crucial baseline for assessing the impact of different orbital sorting strategies, which will be discussed below.

PNOFs provide a convenient polynomial scaling for managing large subspaces compared to traditional active-space wavefunction methods. Still, perfect pairing is a notable case, as it is computationally efficient due to the small subspace size, which allows for fast iterations and accelerates convergence by limiting the degrees of freedom. Therefore, starting with a perfect pairing calculation as an initial guess can be advantageous, followed by expanding the subspace size to expedite the computation. This approach, now labeled the incremental approach, is illustrated in Figure 3. The figure compares two orbital sorting schemes: the previously employed continuous orbital sorting, shown in red, and the newly proposed alternating orbital sorting, represented in blue.

In the continuous orbital sorting scheme, the weakly occupied orbitals are grouped sequentially within subspaces. As a consequence, increasing the subspace size for a new calculation requires modifying the existing subspace structure, redistributing orbitals, and disrupting the previously converged solution. This results in a temporary increase in energy whenever an orbital is added, as the convergence process must restart to adjust to the new

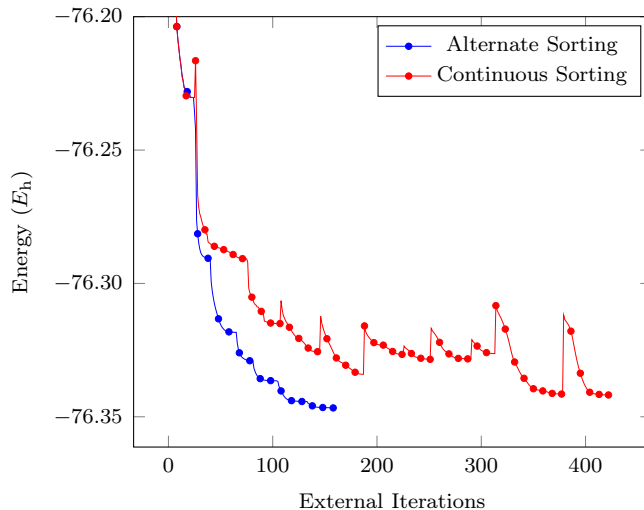


Figure 3: Energy variations in the water molecule during the incremental increase of  $N_g$ , starting with a single weakly occupied orbital ( $N_g = 1$ ) and reaching the maximum value ( $N_g = 12$ ) allowed by the cc-pVTZ basis set.

configuration. This behavior is evident in the red curve of Figure 3, where the energy fluctuates and does not decrease monotonically as the number of coupled orbitals increases.

In contrast, the alternating orbital sorting method circumvents this issue by distributing weakly occupied orbitals across different subspaces in a staggered fashion. This ensures that newly added orbitals do not interfere with the previously established convergence, allowing for a seamless extension of the subspace. The effect of this strategy is reflected in the blue curve of Figure 3, where the energy exhibits a smooth and continuous decrease as more orbitals are incorporated, leading to a more stable and efficient convergence process. Notably, this behavior demonstrates that the new sorting method effectively preserves the information obtained in previous calculations, reducing the computational overhead associated with recalculations.

The improvements achieved with the alternating orbital sorting method translate into a direct gain in computational efficiency. By enabling a smooth and monotonic energy descent, this approach significantly reduces the number of iterations required to reach convergence, compared to continuous orbital sorting. Consequently, the method facilitates a more flexible and scalable strategy for handling large subspaces while maintaining numerical stabil-

ity. The findings presented in Figure 3 highlight the clear advantages of the new sorting approach, making it particularly valuable for studies involving strongly correlated systems that require efficient orbital optimization.

Another key comparison is to assess whether performing a one-shot calculation, where the maximum number of coupled weakly occupied orbitals allowed by the basis set is included from the start, is more efficient than the incremental approach. Unlike incremental calculations, the one-shot method does not rely on previously optimized orbitals and instead starts the optimization from scratch. Since the one-shot calculation is independent of the orbital sorting scheme used to form the subspaces, this comparison is carried out exclusively using the new alternating orbital sorting strategy. The results are presented in Figure 4, which displays two panels: the top panel shows the energy evolution as a function of external iterations, while the bottom panel presents the energy progression as a function of total computational time.

For the one-shot approach, all red marks in Figure 4 correspond to calculations where  $N_g^{\max}$  is used from the beginning. In contrast, the incremental approach, shown in blue, starts with  $N_g = 1$  and progressively increases the number of coupled weakly occupied orbitals until reaching  $N_g^{\max}$ . At first glance, the top panel reveals that the incremental approach requires a significantly larger number of external iterations compared to the one-shot calculation. However, this observation alone does not provide a complete picture as not all iterations contribute equally to the total computational cost. Most of the iterations in the incremental approach are substantially faster than those in the one-shot approach, which is evident in the bottom panel, where the time difference between the two approaches is notably reduced. This suggests that while the incremental approach involves more iterations, its computational efficiency per iteration partially offsets the higher iteration count.

To further investigate possible optimizations, we tested an intermediate strategy labeled the two-step approach, which is represented by green marks in Figure 4. In this method, we begin with a perfect pairing calculation ( $N_g = 1$ ) and then directly transition to  $N_g^{\max}$  without going through the intermediate steps of the incremental approach. The results show that the two-step method offers a clear advantage over the one-shot approach in both the number of iterations and the total computational time. This efficiency gain is attributed to the fact that starting with a perfect pairing solution allows the optimization process to begin from a well-defined reference state,

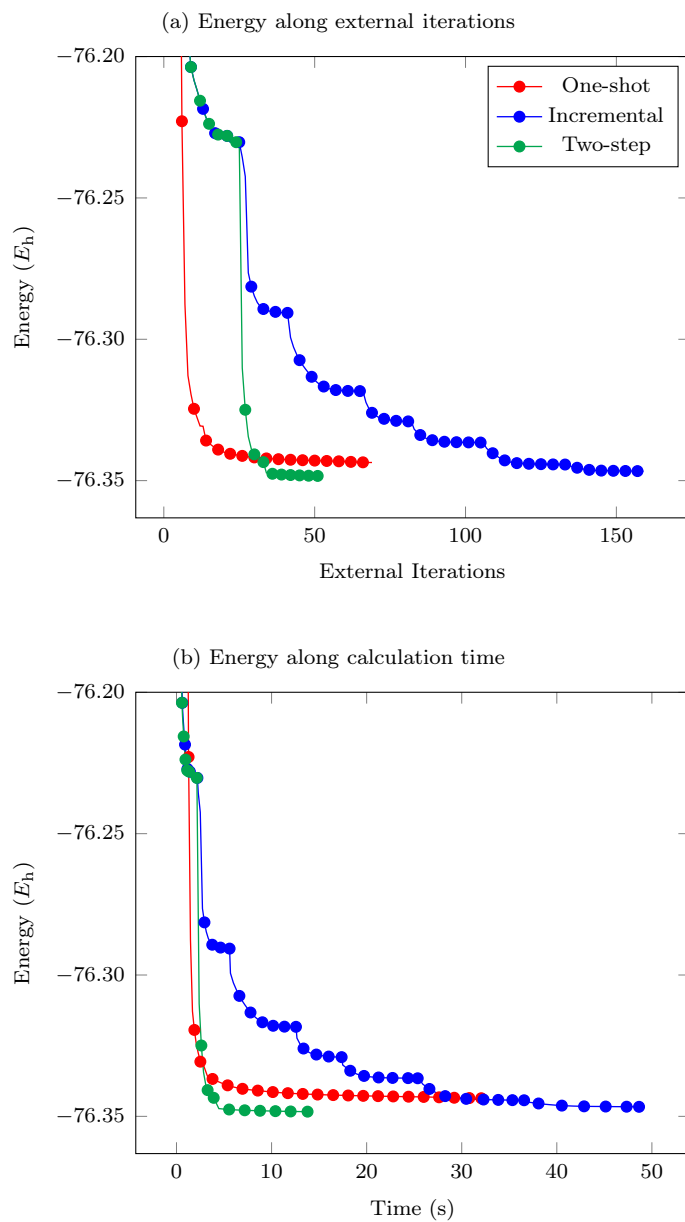


Figure 4: Energy profile along the calculation of  $\text{H}_2\text{O}/\text{cc-pVTZ}$ . One-shot corresponds to a single calculation with the maximum value of  $N_g$  possible, Incremental corresponds to a perfect pairing calculation followed by several restarts including one more orbital on the subspace up to the maximum value of  $N_g$ , and Two-step correspond to a perfect pairing calculation followed by a restart with the maximum value of  $N_g$ .

reducing the complexity of the full optimization problem when the subspace is expanded to  $N_g^{\max}$ .

Overall, the findings from Figure 4 indicate that, while the one-shot approach remains viable, the incremental and two-step approaches offer practical advantages. The incremental approach leverages previously optimized orbitals, leading to smoother convergence and better numerical stability, whereas the two-step approach provides a computationally efficient balance between accuracy and cost. These results demonstrate that by strategically structuring the orbital sorting and optimization process, significant improvements in computational efficiency can be achieved without compromising the accuracy of the electronic structure description.

Additional validation of the different approaches is presented in Figure 5, which examines hydrogen peroxide ( $\text{H}_2\text{O}_2$ ) and ammonia ( $\text{NH}_3$ ) as test cases. These molecules provide a broader perspective on the performance of orbital sorting strategies in chemically distinct systems. Given that our primary objective is to accelerate computations, the discussion focuses on the total computational time required to reach convergence. The top panel of Figure 5 displays the energy evolution as a function of calculation time for  $\text{H}_2\text{O}_2$ , while the bottom panel presents the corresponding results for  $\text{NH}_3$ .

Consistent with previous observations, the incremental approach exhibits a monotonic energy decrease as the subspace size expands, reflecting a smooth and controlled convergence. This behavior is particularly advantageous as it allows the reuse of previously optimized orbitals, leading to improved numerical stability and a reduction in the number of expensive re-optimizations. Notably, this sequential refinement process is only feasible due to the alternating orbital sorting strategy, which preserves the previously converged solution while allowing new orbitals to be incorporated incrementally. Without this sorting scheme, the reordering of orbitals between steps would disrupt the optimization process, increasing the computational cost.

Among the three approaches tested, the two-step strategy, which consists of performing a perfect pairing calculation ( $N_g = 1$ ) followed by an extended pairing calculation with the maximum number of coupled orbitals ( $N_g^{\max}$ ), emerges as the most efficient scheme. As illustrated in Figure 5, this approach consistently achieves the lowest total computation time. The two-step approach leverages an optimized initial reference (perfect pairing) to accelerate convergence when transitioning to the full subspace, thereby outperforming both the incremental and one-shot approaches in terms of efficiency.

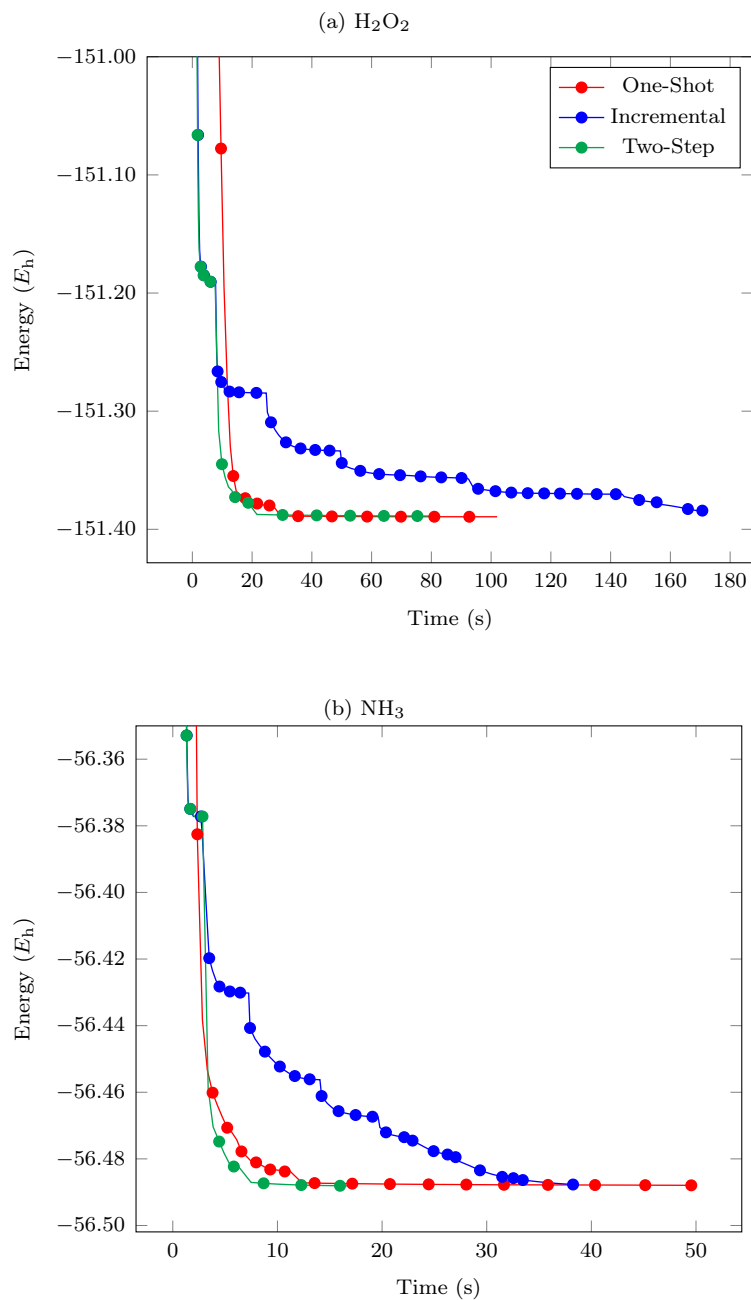


Figure 5: Profile of the energy along the calculation time for the  $\text{H}_2\text{O}_2$  ( $N_g^{\text{max}} = 10$ ) and  $\text{NH}_3$  ( $N_g^{\text{max}} = 15$ ) with the cc-pVTZ basis set, using the One-Shot, the Incremental and the Two-Step approaches.



The results in Figure 5 further support the generality of the proposed sorting and optimization strategies. The efficiency gains observed for  $\text{H}_2\text{O}_2$  and  $\text{NH}_3$  demonstrate that the benefits of the alternating orbital sorting scheme, as well as the incremental and two-step approaches, extend beyond the specific case of water. These findings confirm that the two-step approach is the optimal computational strategy, making it a robust and scalable method for NOF calculations in correlated molecular systems.

#### 4. Conclusion

The introduction of the alternating orbital sorting scheme significantly enhances the computational efficiency and flexibility of the DoNOF program, enabling a more adaptive optimization process that efficiently reuses previously converged solutions. By preserving orbital information across calculations, this approach reduces computational time and improves numerical stability, making it particularly beneficial for systems where computational resources are constrained.

Benchmark calculations on  $\text{H}_2\text{O}$ ,  $\text{H}_2\text{O}_2$ , and  $\text{NH}_3$  confirm that the alternating orbital sorting scheme outperforms previous one-shot approaches, achieving faster convergence while maintaining accuracy. Among the tested strategies, the two-step method emerges as the most efficient, leveraging an optimized initial reference (perfect pairing) to accelerate the transition to the full subspace, thereby reducing overall computational cost. These findings demonstrate that the proposed sorting scheme provides an efficient and scalable framework for improving NOF calculations.

Beyond the current study, the alternating orbital sorting scheme opens new opportunities for extending NOFT to larger and more complex systems. The present results highlight how small orbital subspaces can be strategically used to facilitate faster convergence in larger subspaces within the same basis set. Future work will explore extending this approach by incorporating solutions from small basis sets into calculations with larger basis sets, ultimately improving computational efficiency while ensuring an accurate description of both static and dynamic electron correlations.

#### Acknowledgments

All authors acknowledge the Donostia International Physics Center (DIPC) for its support. E. Boutou thanks Polytech Clermont-Ferrand, the Erasmus

program, and the Auvergne Rhône-Alpes region for funding her internship. J. F. H. Lew-Yee acknowledges the MCIN program "Severo Ochoa" under reference AEI/CEX2018-000867-S for postdoctoral funding (Ref.: 2023/74). This work has received financial support from the Ministry of Science, Innovation, and Universities (MCIU) under project PID2021-126714NB-I00 and from the Basque Government (Eusko Jaurlaritza, IT1584-22). The authors also thank SGIker (UPV/EHU/ERDF, EU) for providing technical and human support, as well as for the allocation of computational resources through the Scientific Computing Service.

## Appendix

Consider a mixed singlet state of  $N$  spin-paired electrons. The Global Natural Orbital Functional (GNOF) follows an electron-pairing approach, where the orbital space  $\Omega$  is divided into  $N/2$  mutually disjoint subspaces  $\Omega_g$ . Each orbital belongs exclusively to a single subspace  $\Omega_g$ , which consists of one strongly double-occupied orbital  $g$  and  $N_g$  weakly double-occupied orbitals. This partitioning ensures that the sum of the occupation numbers within each subspace is exactly two, while maintaining that the trace of the one-particle reduced density matrix correctly corresponds to the total number of electrons.

The reconstruction functional for the two-particle reduced density matrix in terms of the occupation numbers leads to GNOF, as illustrated by the equation:

$$E_{\text{el}} = E^{\text{intra}} + E_{\text{HF}}^{\text{inter}} + E_{\text{sta}}^{\text{inter}} + E_{\text{dyn}}^{\text{inter}} \quad (\text{A1})$$

The intra-pair component is formed by summing the energies of electron pairs, specifically,

$$E^{\text{intra}} = \sum_{g=1}^{N/2} \left[ 2 \sum_{p \in \Omega_g} n_p H_{pp} + \sum_{p, q \in \Omega_g} \Pi(n_q, n_p) L_{pq} \right] \quad (\text{A2})$$

where  $H_{pp}$  are the diagonal one-electron matrix elements of the kinetic energy and external potential operators, whereas  $L_{pq} = \langle pp|qq \rangle$  are the exchange-time-inversion integrals. The matrix elements  $\Pi(n_q, n_p) = c(n_q)c(n_p)$ , where  $c(n_p)$  is defined by the square root of the occupation numbers according to the following rule:

$$c(n_p) = \begin{cases} \sqrt{n_p}, & p \leq N/2 \\ -\sqrt{n_p}, & p > N/2 \end{cases} \quad (\text{A3})$$

that is, the phase factor of  $c(n_p)$  is chosen to be +1 for the strongly occupied orbital of a given subspace  $\Omega_g$ , and  $-1$  otherwise. The inter-subspace Hartree-Fock (HF) term is

$$E_{\text{HF}}^{\text{inter}} = \sum'_{p,q} n_q n_p (2J_{pq} - K_{pq}) \quad (\text{A4})$$

where  $J_{pq} = \langle pq|pq\rangle$  and  $K_{pq} = \langle pq|qp\rangle$  are the Coulomb and exchange integrals, respectively. The prime in the summation indicates that only the inter-subspace terms are taken into account. The inter-subspace static component is written as

$$E_{\text{sta}}^{\text{inter}} = - \sum'_{p,q} (1 - \delta_{q\Omega^b} \delta_{p\Omega^b}) \Phi_q \Phi_p L_{pq} \quad (\text{A5})$$

where  $\Phi_p = \sqrt{n_p h_p}$  with the hole  $h_p = 1 - n_p$ . Finally, the inter-subspace dynamic energy is

$$E_{\text{dyn}}^{\text{inter}} = \sum'_{p,q} (1 - \delta_{q\Omega^b} \delta_{p\Omega^b}) [\Pi(n_q^d, n_p^d) + n_q^d n_p^d] L_{pq} \quad (\text{A6})$$

In Eqs. (A5) and (A6),  $\Omega^b$  denotes the subspace composed of orbitals below the level  $N/2$ , whereas  $n_p^d$  is the dynamic part of the occupation number  $n_p$  in accordance with the Pulay's criterion that establishes an occupancy deviation of approximately 0.01 with respect to 1 or 0 for a natural orbital to contribute to the dynamic correlation.

## References

- [1] T. L. Gilbert, Hohenberg-kohn theorem for nonlocal external potentials, Phys. Rev. 12 (6) (1975) 2111–2120. doi:10.1103/PhysRevB.12.2111.
- [2] R. A. Donnelly, R. G. Parr, Elementary properties of an energy functional of the first-order reduced density matrix, J. Chem. Phys. 69 (1978) 4431–4439. doi:10.1063/1.436433.
- [3] R. A. Donnelly, On fundamental difference between energy functionals based on first- and second-order density matrices, J. Chem. Phys. 71 (1979) 2874–2879. doi:10.1063/1.438678.

- [4] M. Levy, Universal variational functionals of electron densities, first-order density matrices, and natural spin-orbitals and solution of the  $v$ -representability problem, *Proc. Natl. Acad. Sci. USA* 76 (12) (1979) 6062–6065. doi:10.1088/0022-3719/12/3/015.
- [5] S. M. Valone, Consequences of extending 1 matrix energy functionals pure-state representable to all ensemble representable 1 matrices, *J. Chem. Phys.* 73 (3) (1980) 1344–1349. doi:10.1063/1.440249.
- [6] M. Piris, Exploring the potential of natural orbital functionals, *Chemical Science* 15 (2024) 17284–17291. doi:10.1039/d4sc05810k.
- [7] J. F. H. Lew-Yee, M. Piris, J. M. del Campo, Resolution of the identity approximation applied to pnof correlation calculations, *J. Chem. Phys.* 154 (2021) 064102. doi:10.1063/5.0036404.
- [8] Y. Lemke, J. Kussmann, C. Ochsenfeld, Efficient integral-direct methods for self-consistent reduced density matrix functional theory calculations on central and graphics processing units, *J. Chem. Theory Comput.* 18 (2022) 4229–4244. doi:10.1021/acs.jctc.2c00231.
- [9] J. F. H. Lew-Yee, J. M. del Campo, M. Piris, Electron correlation in the iron(ii) porphyrin by natural orbital functional approximations, *J. Chem. Theory Comput.* 19 (2023) 211–220. doi:10.1021/acs.jctc.2c01093.
- [10] X. Lopez, F. Ruipérez, M. Piris, J. M. Matxain, J. M. Ugalde, Diradicals and diradicaloids in natural orbital functional theory., *ChemPhysChem* 12 (2011) 1061–1065. doi:10.1002/cphc.201100136.
- [11] F. Ruipérez, M. Piris, J. M. Ugalde, J. M. Matxain, The natural orbital functional theory of the bonding in  $cr(2)$ ,  $mo(2)$  and  $w(2)$ ., *Phys. Chem. Chem. Phys.* 15 (2013) 2055–2062. doi:10.1039/c2cp43559d.
- [12] E. Ramos-Cordoba, X. Lopez, M. Piris, E. Matito, H4: A challenging system for natural orbital functional approximations, *J. Chem. Phys.* 143 (2015) 164112. doi:10.1063/1.4934799.
- [13] I. Mitxelena, M. Piris, M. Rodriguez-Mayorga, M. A. R. Mayorga, On the performance of natural orbital functional approximations in hubbard model, *J. Phys.: Cond. Matt.* 29 (2017) 425602. doi:10.1088/1361-648X/aa80ca.

- [14] X. Lopez, M. Piris, Performance of the nof-mp2 method in hydrogen abstraction reactions, *Theor. Chem. Acc.* 138 (2019) 89. doi:10.1007/s00214-019-2475-5.
- [15] I. Mitxelena, M. Piris, An efficient method for strongly correlated electrons in one dimension, *J. Phys.: Cond. Matt.* 32 (2020) 17LT01. doi:10.1088/1361-648X/ab6d11.
- [16] I. Mitxelena, M. Piris, An efficient method for strongly correlated electrons in two-dimensions, *J. Chem. Phys.* 152 (2020) 064108. doi:10.1063/1.5140985.
- [17] I. Mitxelena, M. Piris, Benchmarking gnof against fci in challenging systems in one, two, and three dimensions, *J. Chem. Phys.* 156 (2022) 214102. doi:10.1063/5.0092611.
- [18] I. Mitxelena, M. Piris, Assessing the global natural orbital functional approximation on model systems with strong correlation, *J. Chem. Phys.* 160 (2024) 204106–8. doi:10.1063/5.0207325.
- [19] K. Chatterjee, K. Pernal, Excitation energies from extended random phase approximation employed with approximate one- and two-electron reduced density matrices, *J. Chem. Phys.* 137 (2012) 204109. doi:10.1063/1.4766934.
- [20] J. F. H. Lew-Yee, I. A. Bonfil-Rivera, M. Piris, J. M. del Campo, Excited states by coupling piris natural orbital functionals with the extended random-phase approximation, *J. Chem. Theory Comput.* 20 (2024) 2140–2151. doi:10.1021/acs.jctc.3c01194.
- [21] A. Rivero-Santamaría, M. Piris, Time evolution of natural orbitals in ab initio molecular dynamics, *J. Chem. Phys.* 160 (2024) 071102. doi:10.1063/5.0188491.
- [22] M. Piris, X. Lopez, J. M. Ugalde, Time-resolved chemical bonding structure evolution by direct-dynamics chemical simulations, *J. Phys. Chem. Lett.* (2024) 12138–12143. doi:10.1021/acs.jpcllett.4c03010.
- [23] J. F. H. Lew-Yee, M. Piris, J. M. Campo, Outstanding improvement in removing the delocalization error by global natural orbital functional, *J. Chem. Phys.* 158 (2023) 084110. doi:10.1063/5.0137378.

- [24] J. F. H. Lew-Yee, J. M. del Campo, M. Piris, Advancing Natural Orbital Functional Calculations Through Deep Learning-Inspired Techniques for Large-Scale Strongly Correlated Electron Systems, *Phys. Rev. Lett.* (2025). doi:10.48550/arXiv.2411.18493.
- [25] P. O. Löwdin, Quantum Theory of Many-Particle Systems. I. Physical Interpretations by Means of Density Matrices, Natural Spin-Orbitals, and Convergence Problems in the Method of Configurational Interaction, *Phys. Rev.* 97 (1955) 1474–1489. doi:10.48550/10.1103/PhysRev.97.1474.
- [26] M. Piris, Natural Orbital Functional Theory, in *Reduced-Density-Matrix Mechanics: With Applications to many-electron atoms and molecules*, edited by D. A. Mazziotti, *Advances in Chemical Physics*, Vol. 134, Ch. 14, pp. 387–427, John Wiley and Sons, Hoboken, New Jersey, USA, 2007. doi:10.48550/10.1002/0470106603.
- [27] K. Pernal, K. J. H. Giesbertz, Reduced density matrix functional theory (rdmft) and linear response time-dependent rdmft (td-rdmft), *Top Curr Chem* 368 (2016) 125–184. doi:10.1007/128\_2015\_624.
- [28] R. Schade, E. Kamil, P. Blöchl, Reduced density-matrix functionals from many-particle theory, *Eur. Phys. J. Spec. Top.* 226 (2017) 2677–2692. doi:10.1140/epjst/e2017-70046-0.
- [29] M. Piris, Advances in approximate natural orbital functionals: From historical perspectives to contemporary developments, *Adv. Quantum Chem.* 90 (2024) 15–66. doi:10.1016/bs.aiq.2024.04.002.
- [30] M. Piris, A new approach for the two-electron cumulant in natural orbital, *Int. J. Quantum Chem.* 106 (2006) 1093–1104. doi:10.1002/qua.20858.
- [31] M. Piris, X. Lopez, J. M. Ugalde, Dispersion interactions within the Piris natural orbital functional theory: the helium dimer, *J. Chem. Phys.* 126 (2207) 214103. doi:10.1063/1.2743019.
- [32] M. Piris, J. M. Matxain, X. Lopez, J. M. Ugalde, Communications: Accurate description of atoms and molecules by natural orbital functional theory, *J. Chem. Phys.* 132 (2010) 031103. doi:10.1063/1.3298694.

- [33] M. Piris, J. M. Matxain, X. Lopez, J. M. Ugalde, Communications: The role of the positivity N-representability conditions in natural orbital functional theory, *J. Chem. Phys.* 133 (2010) 111101. doi:10.1063/1.3481578.
- [34] M. Piris, X. Lopez, F. Ruipérez, J. M. Matxain, J. M. Ugalde, A natural orbital functional for multiconfigurational states., *J. Chem. Phys.* 134 (2011) 164102. doi:10.1063/1.3582792.
- [35] M. Piris, J. M. Matxain, X. Lopez, The intrapair electron correlation in natural orbital functional theory, *J. Chem. Phys.* 139 (2013) 234109. doi:10.1063/1.4844075.
- [36] M. Piris, Interacting pairs in natural orbital functional theory, *J. Chem. Phys.* 141 (2014) 044107. doi:10.1063/1.4890653.
- [37] M. Piris, Global method for electron correlation, *Phys. Rev. Lett.* 119 (2017) 063002–5. doi:10.1103/PhysRevLett.119.063002.
- [38] I. Mitxelena, M. Rodríguez-Mayorga, M. Piris, “Phase Dilemma in Natural Orbital Functional Theory from the N-representability Perspective”, *Eur. Phys. J. B* 91 (2018) 109. doi:10.1140/epjb/e2018-90078-8.
- [39] M. Piris, Global natural orbital functional: Towards the complete description of the electron correlation, *Physical Review Letters* 127 (2021) 233001. doi:10.1103/PhysRevLett.127.233001.
- [40] M. Piris, The role of the N-representability in one-particle functional theories, Springer, 2018, pp. 261–278. doi:10.1007/978-3-319-72374-7\_22.
- [41] T. T. Nguyen-Dang, E. V. Ludena, Y. Tal, Variation of the energy functional of the reduced first-order density operator, *J. Mol. Struct.: THEOCHEM* 120 (1985) 247–264. doi:10.1016/0166-1280(85)85114-9.
- [42] C. Schilling, Communication: Relating the pure and ensemble density matrix functional, *J. Chem. Phys.* 149 (2018) 231102. doi:10.1063/1.5080088.

- [43] G. V. Oleg, K. Pernal, Approximating one-matrix functionals without generalized Pauli constraints, *Phys. Rev. A* 100 (2019) 012509. doi:10.1103/PhysRevA.100.012509.
- [44] K. Husimi, Some formal properties of the density matrix, *Proc. Phys. Math. Soc. Jpn.* 22 (1940) 264–314. doi:10.11429/ppmsj1919.22.4\_264.
- [45] D. A. Mazziotti, Structure of fermionic density matrices: Complete n-representability conditions, *Phys. Rev. Lett.* 108 (2012) 263002. doi:10.1103/PhysRevLett.108.263002.
- [46] M. Piris, A generalized self-consistent-field procedure in the improved BCS theory, *J. Math. Chem.* 25 (1999) 47–54. doi:10.1023/A:1019111828412.
- [47] M. Rodríguez-Mayorga, P. F. Loos, F. Bruneval, L. Visscher, Time-Reversal Symmetry in RDMFT and pCCD with Complex-Valued Orbitals, arXiv:2410.03620. doi:10.48550/arXiv.2410.03620.
- [48] M. Piris, A natural orbital functional based on an explicit approach of the two-electron cumulant, *Int. J. Quantum Chem.* 113 (2013) 620–630. doi:10.1002/qua.24020.
- [49] M. Piris, J. M. Ugalde, Perspective on natural orbital functional theory, *Int. J. Quantum Chem.* 114 (2014) 1169–1175. doi:10.1002/qua.24663.  
URL <http://doi.wiley.com/10.1002/qua.24663>
- [50] I. Mitxelena, M. Piris, J. J. M. Ugalde, Advances in approximate natural orbital functional theory, Vol. 79, Academic Press, 2019, pp. 155–177. doi:<https://doi.org/10.1016/bs.aiq.2019.04.001>.
- [51] M. Piris, The Electron Pairing Approach in Natural Orbital Functional Theory, Apple Academic Press, 2018, pp. 593–620. doi:10.1201/9781351170963.
- [52] M. Piris, I. Mitxelena, DoNOF: An open-source implementation of natural-orbital-functional-Comput. Phys. Commun. 259 (2021) 107651.  
URL <https://github.com/DoNOF/DoNOFsw>



- [53] A. J. Coleman, Structure of Fermion Density Matrices, *Rev. Mod. Phys.* 35 (1963) 668–687. doi:10.1103/RevModPhys.35.668.
- [54] M. Piris, J. M. Ugalde, Iterative diagonalization for orbital optimization in natural orbital functional theory, *J. Comput. Chem.* 30 (2009) 2078–2086. doi:10.1002/jcc.21225.
- [55] L. Franco, I. A. Bonfil-Rivera, J. F. Huan Lew-Yee, M. Piris, J. M Del Campo, R. A. Vargas-Hernández, Softmax parameterization of the occupation numbers for natural orbital functionals based on electron pairing approaches, *J. Chem. Phys.* 160 (2024) 244107. doi:10.1063/5.0213719.
- [56] M. Piris, Natural orbital functional for multiplets, *Phys. Rev. A* 100 (2019) 32508. doi:10.1103/PhysRevA.100.032508.
- [57] T. H. Dunning, T. H. D. Jr., Gaussian basis sets for use in correlated molecular calculations. i. the atoms boron through neon and hydrogen, *J. Chem. Phys.* 90 (1989) 1007–1023. doi:10.1063/1.456153.